INFECTION AND IMMUNITY, Nov. 2010, p. 4488–4499 Vol. 78, No. 11
0019-9567/10/$12.00 doi:10.1128/IAI.00620-10
Copyright © 2010, American Society for Microbiology. All Rights Reserved.

Human Intestinal Tissue and Cultured Colonic Cells Contain Globotriaosylceramide Synthase mRNA and the Alternate Shiga Toxin Receptor Globotetraosylceramide▽

Steven D. Zumbrun,[1] Leanne Hanson,[1] James F. Sinclair,[1] James Freedy,[1] Angela R. Melton-Celsa,[1] Jaime Rodriguez-Canales,[2] Jeffrey C. Hanson,[2] and Alison D. O'Brien[1]*

Department of Microbiology and Immunology, Uniformed Services University of the Health Sciences, Bethesda, Maryland 20814,[1] *and Laser Capture Microdissection Core Facility, Laboratory of Pathology, National Cancer Institute, National Institutes of Health, Bethesda, Maryland 20814*[2]

Received 8 June 2010/Returned for modification 5 July 2010/Accepted 12 August 2010

***Escherichia coli* O157:H7 and other Shiga toxin (Stx)-producing *E. coli* (STEC) bacteria are not enteroinvasive but can cause hemorrhagic colitis. In some STEC-infected individuals, a life-threatening sequela of infection called the hemolytic uremic syndrome may develop that can lead to kidney failure. This syndrome is linked to the production of Stx by the infecting organism. For Stx to reach the kidney, the toxin must first penetrate the colonic epithelial barrier. However, the Stx receptor, globotriaosylceramide (Gb3), has been thought to be absent from human intestinal epithelial cells. Thus, the mechanisms by which the toxin associates with and traverses through the intestine en route to the kidneys have been puzzling aspects of STEC pathogenesis. In this study, we initially determined that both types of Stx made by STEC, Stx1 and Stx2, do in fact bind to colonic epithelia in fresh tissue sections and to a colonic epithelial cell line (HCT-8). We also discovered that globotetraosylceramide (Gb4), a lower-affinity toxin receptor derived from Gb3, is readily detectable on the surfaces of human colonic tissue sections and HCT-8 cells. Furthermore, we found that Gb3 is present on a fraction of HCT-8 cells, where it presumably functions to bind and internalize Stx1 and Stx2. In addition, we established by quantitative real-time PCR (qRT-PCR) that both fresh colonic epithelial sections and HCT-8 cells express Gb3 synthase mRNA. Taken together, our data suggest that Gb3 may be present in small quantities in human colonic epithelia, where it may compete for Stx binding with the more abundantly expressed glycosphingolipid Gb4.**

Shiga toxins (Stxs) are highly potent ribotoxic virulence factors associated with the worst pathological manifestations of infection by *Escherichia coli* serotype O157:H7 and other Stx-producing *E. coli* (STEC) bacteria. Two major types of Stxs are produced by STEC, Stx1 and Stx2, and an organism may produce one or both toxins. Stx1 and Stx2 share enzymatic and structural features but are immunologically distinct. More than 110,000 cases of STEC infection are estimated to occur each year in the United States, and about 75,000 of those cases are caused by *E. coli* O157:H7 infection. Many individuals infected with *E. coli* O157:H7 present with severe abdominal pain and bloody diarrhea, of which the latter may be caused by the action of Stxs on endothelial cells that line the small blood vessels (microvasculature) in the gastrointestinal tract (4, 26, 42, 44). In some patients, STEC infection leads to a serious sequela called the hemolytic uremic syndrome (HUS). The HUS is characterized by a triad of clinical features that include thrombocytopenia, hemolytic anemia, and acute kidney failure, and it occurs most frequently in children less than 10 years of age (2, 12). Of note, HUS associated with *E. coli* O157:H7 infection is a major cause of acute kidney failure in children in the United States and worldwide (6, 61). One hypothesis for how the renal injury occurs in HUS is that blood-borne Stx induces apoptosis in endothelial cells in the glomerular microvasculature (19). Thrombi then form in these damaged blood vessels, a characteristic pathological feature of the HUS. Death of renal tubular cells has also been linked to Stx production in humans and in mouse models of *E. coli* O157:H7 infection (7, 34, 56).

How Stx moves from the lumen of the bowel to the blood vessels that lie below the surface of the gastrointestinal tract to reach the kidneys has not been determined. Presumably, the toxin breaches the epithelial barrier of the colon at or near the site of colonization by the noninvasive *E. coli* O157:H7. However, the colonic epithelium has been reported to lack globotriaosylceramide (Gb3), the established and preferred receptor for Stx1 and Stx2. The consensus in the literature that the Stx receptor, Gb3, is not present in the human colonic epithelial cells was originally based on conclusions that were drawn from analysis of the general glycolipid composition of the human large intestine (17, 52). In those studies, glycolipids from either mucosal scrapes or the entire mucosal layer were examined by thin-layer chromatography (TLC). Although these mucosal specimens were reported to contain small but measurable levels of Gb3, the samples included not only epithelial cells but also Gb3-enriched endothelial cells. Therefore, evidence of the presence of Gb3 on the cell surface of large bowel epithelial cells was inconclusive. In another investigation, trace amounts of Gb3 were found in epithelial cells isolated by sequential washes of colon tissue with buffer that contained EDTA and

* Corresponding author. Mailing address: Department of Microbiology and Immunology, Uniformed Services University of the Health Sciences, 4301 Jones Bridge Road, Bethesda, MD 20814-4799. Phone: (301) 295-3419. Fax: (301) 295-3773. E-mail: aobrien@usuhs.mil.

▽ Published ahead of print on 23 August 2010.

reducing agent to gently remove cells layer by layer; however, again, nonepithelial cell contamination could not be ruled out (16). Holgersson et al. ultimately concluded that large bowel epithelial cells do not express "glycolipid-borne Galα1-4 Gal sequence" (components of Gb3) based on the failure to detect Gb3 on the cell surface with Gb3-specific antibody (16). Nevertheless, some of these early studies do suggest that Gb3 may be present in trace amounts in colonic epithelia. These findings, however, appear to have been discounted by many in the field, who assert, based on the negative immunodetection by Holgersson et al. described above (16) and findings of subsequent studies (36, 48), that Gb3 is not present on the colonic epithelium (29).

Given the presumed lack of colonic epithelial Gb3, a number of theories have been promulgated to explain how Stx is able to penetrate the epithelial barrier to reach the bloodstream (29). Two related hypotheses are as follows: (i) Stx follows a paracellular course and moves between cells during immune cell infiltration that follows infection (55), or (ii) Stx transits to the bloodstream from the bowel lumen through possible "holes" in the mucosa that result from attachment-and-effacement (A&E) lesions and Stx damage (33). A third hypothesis is that Stx moves by a transcellular route from the lumen to the vasculature in the lamina propria, such as through an alternative but undefined trafficking pathway that does not involve Gb3. In support of the latter conjecture, Stx was found to transcytose polarized tissue culture cells that appeared to lack Gb3 in the absence of cellular damage (1). However, in a human organ culture model, Stx-mediated intestinal epithelial damage was observed (48), a finding that seems to support the second hypothesis above. A fourth premise to explain how Stx crosses the mucosal barrier in the absence of Gb3 on enterocytes is that an alternative receptor exists (11). Such a putative receptor could either mediate Stx-induced cytotoxicity and thus cause a breach in the epithelial barrier or allow transcellular movement of the toxin across the epithelial cell. However, evidence in support of an alternative receptor to Gb3 is not strong. Rather, accumulated data suggest that Gb3 is the sole functional receptor for all Stxs (19, 22, 24, 27, 32, 34, 40, 43, 50, 51, 59), and they can be summarized by 4 lines of evidence. First, cellular cytotoxicity is directly proportional to cell surface Gb3 content (21, 46, 47). Second, Gb3 provided to resistant cells via liposomes induces Stx1 sensitivity in those cells, whereas Gb4 does not (58). Third, Gb3 expression appears to correlate with clinical manifestations of STEC disease. The highest Gb3 content is found in the microvascular glomeruli and proximal tubule cells of the kidney, consistent with renal pathology in HUS (41). Other Gb3-rich regions include the colonic microvascular endothelia, with its associated lamina propria (bloody colitis) (21), and endothelial vasculature of the cerebellum (neurological symptoms) (46). This link between high Gb3 content and Stx toxicity is also seen in animal models. In rabbits, intravenous administration of Stx1 or Stx2 produces vascular lesions in those tissues with high concentrations of Gb3, i.e., the intestine and the central nervous system (47). Furthermore, rabbit kidneys lack Gb3, and no tissue injury is observed there (7). Fourth, Gb3 synthase knockout mice are resistant to Stx effects, although in these mice, other glycosphingolipids, including Gb4, are eliminated as well (43).

In this study, we asked whether Stxs could bind to sections of human colonic epithelia and if so by what receptor(s). Based on our initial observation that small amounts of Stx1 and Stx2 were capable of binding to the surface of colonic epithelia, we investigated the possibility that small amounts of Gb3 are present on colonic epithelial cells. Here we present the novel finding that Gb3 synthase mRNA can be detected in epithelial cells isolated by laser capture microdissection (LCM) from normal human colonic tissue sections and that Gb4, a glycosphingolipid derived from Gb3 (Fig. 1), is expressed in this tissue. Furthermore, we demonstrate that while both Stx1 and Stx2 can bind to the epithelial surfaces of those normal human colonic tissue sections, Stx1 binds at relatively higher levels. In addition, we demonstrate that the cytotoxicity of Stx1 and Stx2 for the human colonic cell line HCT-8 can be enhanced 20- to 60-fold by genetically manipulating the cells to increase the cell surface Gb3 content. Collectively, these data suggest that small amounts of Gb3 may mediate Stx uptake in normal colonic

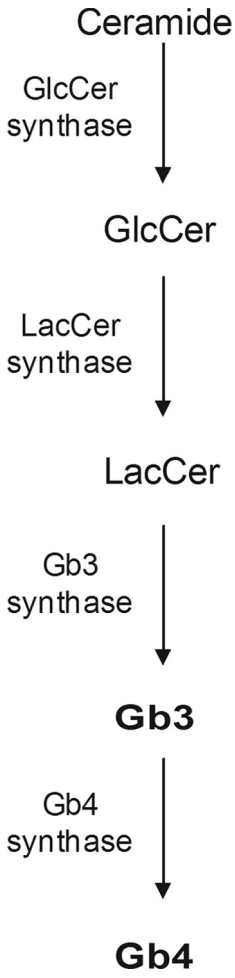

FIG. 1. Globotetraosylceramide (Gb4) synthesis pathway (38). The synthesis of Gb4 requires globotriaosylceramide (Gb3) as a substrate. Biosyntheses of Gb3 and Gb4 are accompanied by intracellular transport, presumably by a vesicle-bound exocytotic membrane flow, from the endoplasmic reticulum (ER) through the Golgi cisternae to the plasma membrane (57). Abbreviations: LacCer, lactose-ceramide; GlcCer, glucose-ceramide.

tissue, an event that leads to cell death, and that abundant Gb4 may compete with Gb3 for Stx binding.

MATERIALS AND METHODS

Toxins. Stx1 and Stx2 were purified by immunoaffinity chromatography from supernatants of *E. coli* K-12 strains carrying recombinant plasmids that encode the toxins (39).

Maintenance and transfection of cell lines. A human colorectal carcinoma cell line, HCT-8 (American Type Culture Collection [ATCC], Manassas, VA), was maintained in RPMI-1640 medium (ATCC). Vero cells were maintained in Eagle's minimal essential medium (EMEM) (Lonza, Inc., Walkersville, MD). Phoenix cells, a retroviral packaging cell line, were maintained in Dulbecco's modified Eagle's medium (DMEM) (Lonza). All media were supplemented with 10% heat-inactivated fetal bovine serum (FBS) (Life Technologies, Carlsbad, CA), penicillin (10 U/ml), gentamicin (100 μg/ml), and streptomycin (10 μg/ml). Cells were grown at 37°C in a 5% CO_2 atmosphere. To generate the stable HCT-8 Gb4 synthase RNA interference (RNAi) knockdown cell line, HCT-8 cells were infected with small hairpin RNA (shRNA)-containing retroviral particles from the supernatant of transfected Phoenix cells. Four different plasmids that contained 29-mer shRNAs against Gb4 synthase mRNA (B3GALNT1, HuSH constructs; Origene, Rockville, MD) were transfected separately into Phoenix cells, following the manufacturer's protocol. The Phoenix cells are a "packaging" cell line used to generate infectious retroviral particles that contain the shRNA. The four *Gb4 synthase* mRNA-complementary shRNA target sequences that we tried are as follows: CGAGTAGGATGTCACTGAGATCCC TCAAA, CACACTTCGAGAGCATTCAAACTGCTCTC, AGGAGTATCCT TTCAAGGTGTTCCCTCCA, and TGTCTGTCAACTGAGACGTGTGATTG CAG. Following the transfection step, cells were grown in RPMI-1640 supplemented with 1 μg/ml puromycin for 4 days until they were 90% confluent. Next, the medium was replaced with RPMI-1640 supplemented with 10% FBS, and the cells were incubated at 37°C in a 5% CO_2 atmosphere for 12 h. The culture supernatants that contained retroviral particles were harvested, and 4 μg/ml polybrene (Sigma-Aldrich, Inc., St. Louis, MO) was added to increase retroviral infectivity. The supernatants were overlaid on HCT-8 cells grown to about 50% confluence and were incubated for 24 h to permit retroviral infection of HCT-8 cells. The culture medium was then replaced with RPMI-1640 supplemented with 10% FBS and 7.5 μg/ml puromycin to maintain selection against HCT-8 cells that did not contain integrated retroviral nucleic acid. The transfected cells were maintained for 2 weeks, and individual cells were isolated by a cloning disk procedure to generate clonally pure, stable cell lines (5).

Antibodies. Primary antibodies used in this study included the following: mouse monoclonal IgG 1A1 anti-StxA1, developed and characterized in this laboratory (unpublished results), mouse monoclonal IgG 13C4 anti-Stx1B (53), mouse monoclonal IgG 11F11 anti-StxA2 (45), rabbit polyclonal anti-Stx1 (unpublished), rabbit polyclonal anti-Stx2 (60), rat monoclonal IgM CD77 anti-Gb3 (GeneTex, Inc., Irvine, CA), and rabbit polyclonal GL-4 anti-Gb4 (Matreya LLC, Pleasant Gap, PA). Secondary antibodies used were as follows: Alexa Fluor 488 goat anti-mouse IgG, Alexa Fluor 488 goat anti-rat IgM, Alexa Fluor 488 goat anti-rabbit IgG, (Life Technologies), and horseradish peroxidase (HRP)-conjugated goat anti-rabbit Ig (Bio-Rad, Hercules, CA).

Immunofluorescent staining of human tissue. Two normal human colonic tissue specimens obtained from an 18-year-old male donor (Biochain, Inc., Hayward, CA) and a 74-year-old male donor (Bioserve, Inc., Beltsville, MD) were used to assess Gb3 and Gb4 levels and to determine Stx1 and Stx2 binding patterns. Tissue specimens were either serially sectioned and acetone fixed on glass slides (Biochain) or sectioned (6 μm) from fresh tissue (Bioserve) and fixed to slides; both sets of slides were frozen for later use. The slides were thawed, blocked with FBS, and incubated with 2 μg of either Stx1 or Stx2 for 1 h at room temperature. The sections were washed with phosphate-buffered saline (PBS) and fixed with 10% percent formalin, and the bound toxin was detected with a cognate mouse monoclonal primary antibody (diluted 1:50 in PBS) and an Alexa Fluor 488 anti-mouse IgG secondary antibody (1:250 dilution in PBS). For Stx1 and Stx2 detection, tissue sections were blocked as above, and then a 1:1 mixture of monoclonal anti-StxA1–anti-Stx1B (1A1-13C4) at a 1:50 dilution in PBS was used to detect Stx1, whereas monoclonal 11F11 anti-StxA2 (1:50) was added to detect Stx2. Sections were incubated with primary antibody overnight at room temperature. Sections were washed with PBS, and Gb3 or Gb4 was detected with an Alexa Fluor 488-conjugated anti-mouse IgG secondary antibody (1:250 dilution in PBS). To delineate individual cells within the tissue, sections were counterstained with 0.01% Evans blue dye for 5 min, followed by extensive washing with PBS.

Immunofluorescent staining of cells. To detect levels of Gb3 and Gb4 on the surfaces of HCT-8 cells and Vero cells, 1×10^5 cells/ml were seeded onto glass coverslips in a 6-well dish (3 ml/well) and grown to ~75% confluence. The seeded wells were gently washed with PBS and then blocked with PBS containing 3% bovine serum albumin (BSA) for 30 min. Rat monoclonal anti-Gb3 (diluted 1:50 in PBS), rabbit polyclonal anti-Gb4 (diluted 1:50 in PBS), or PBS (negative control) was added to the appropriate wells, and specimens were incubated overnight at 37°C. The cells were then washed three times with PBS. The cognate secondary Alexa Fluor 488 antibody was added (diluted 1:250 in PBS) to each coverslip and incubated for 30 min at room temperature. Cells were washed three times with PBS and counterstained with 0.01% Evans blue dye. The stained cells were assessed with a BX60 fluorescent microscope (Olympus, Center Valley, PA). Binding of Stx1 or Stx2 to cells was determined by incubation with Stx1 or Stx2 (200 ng/ml PBS) for 1 h. Samples were blocked with 3% BSA, washed three times with PBS, and fixed for 10 min with 10% percent formalin. Staining of cells was then carried out as described above for sections of human colon.

Flow cytometry. HCT-8 cells were grown to near confluence in T-75 flasks, washed once with PBS, and detached from each flask by incubation with 3 ml 0.05% trypsin-EDTA (Life Technologies) for 20 min at 37°C. Clumps of cells were dispersed by two passages through a 25-gauge needle. Next, cells were counted with a hemocytometer by a standard method. Aliquots of 3×10^6 cells were incubated at 4°C for 30 min in 1.5-ml microcentrifuge tubes and then pelleted by centrifugation. The prechilled cells were resuspended in 0.3 ml of a 1:50 dilution of anti-Gb3 or anti-Gb4 in 4% BSA in PBS (BSA-PBS) and further incubated at 4°C for 1 h. Cells were pelleted by centrifugation, washed once with 0.7 ml cold BSA-PBS, resuspended in 0.3 ml cognate secondary Alexa Fluor antibody (5 μg/ml in PBS), and incubated at 4°C for 30 min with end-over-end rotation. Finally, cells were washed once with 0.7 ml cold BSA-PBS, pelleted by centrifugation, and fixed in 0.5 ml 1% paraformaldehyde in BSA-PBS. The stained and fixed cells were analyzed with an LRS II flow cytometer (BD Biosciences, Franklin Lakes, NJ).

HCT-8 glycolipid extraction and analysis. HCT-8 cells were seeded in tissue culture flasks and grown at 37°C in an atmosphere of 5% CO_2 until the cells were nearly confluent. Adherent cell monolayers were released from the flask by trypsinization as described above, collected by centrifugation, and resuspended in 0.75 ml PBS. The HCT-8 lipids were extracted overnight at room temperature by mixing the cell suspension with chloroform-methanol (2:1 ratio). The aqueous phase was discarded, and the organic phase with extracted lipids was allowed to air dry. The concentrated lipid fraction was suspended in a small volume of chloroform-methanol (2:1 ratio) for further processing. HCT-8 lipids were separated by normal-phase high-performance liquid chromatography (HPLC), following a previously described method (23) with slight modifications. Extracted material (0.025 ml) was injected onto a Lichrosorb silica HPLC column (ES Industries, West Berlin, NJ) and eluted with a mixture of isopropanol (Mallinckrodt Baker, Inc., Phillipsburg, NJ), hexane (optical grade; Fisher Scientific, Pittsburgh, PA), and water applied in a linear gradient with starting and ending ratios of 50:50:1 and 55:40:5, respectively, for each solvent. Eluted material was collected in 20 separate fractions of 1.5 ml each over a 30-min period. Fractions were dried using a speed-vac and resuspended in 0.02 ml of chloroform-methanol (2:1 ratio). A sample of each HPLC fraction was applied to the bottom of a silica gel sheet (EMD Chemicals, Inc., Gibbstown, NJ), and fractionated lipids were subjected to TLC in a glass tank with a mixture of chloroform, methanol, and water (65:35:8). A purified glycosphingolipid standard (Matreya) was also added to the plate for comparison. After the solvent front reached the top of the plate, the gel matrix was air dried and treated with orcinol (Acros Organics, Morris Plains, NJ) to visualize the separated carbohydrate and glycolipid components of each fraction. Fractions that appeared to contain Gb3 and Gb4 based on glycolipid mobility in TLC were subjected to mass spectral analysis to positively identify the molecules. For each HPLC fraction analyzed, 1 μl was applied to a matrix-assisted laser desorption ionization (MALDI) slide (Applied Biosystems, Carlsbad, CA) along with 5 to 10 mg/ml gentisic acid (Sigma-Aldrich) as the energy-absorbing molecule. MALDI–time-of-flight (TOF) mass spectrometry was performed with a Voyager-DE STR mass spectrometer (Applied Biosystems). Analysis of the spectra was accomplished with the software program Explorer (Applied Biosystems).

ELISA to detect Stx binding to purified Gb3 and Gb4. Purified Gb3 or Gb4 glycosphingolipids (Matreya) in 100% ethanol were deposited in wells of a 96-well Immobilon 2HB plate and dried overnight in a laminar flow hood. Wells were washed in 0.1 ml PBST (1× PBS, 0.05% Tween) at 4°C for 1 h, the wash in each well was decanted, and unbound sites on each well were blocked by addition of 0.2 ml PBST-Block (PBST and 3% BSA). Plates were incubated at 4°C for 2 h, and wells were washed twice with 0.15 ml PBST–0.2% BSA per well. Stx1 or Stx2 (20 ng) was added in PBST–0.2% BSA (0.1 ml per well) and incubated for 1 h

at room temperature. Wells were washed three times with 0.2 ml PBST–0.2% BSA before addition of 0.1 ml rabbit polyclonal anti-Stx1 or anti-Stx2 antibody (1:5,000 in PBS). Plates were incubated for 1 h at room temperature. After each well was washed three times with 0.2 ml PBST–0.2% BSA, 0.1 ml goat anti-rabbit-HRP antibody (diluted 1:2,000 in PBS) was added to each well. Plates were incubated for 1 h at room temperature. Again, each well was washed three times with 0.2 ml PBST–0.2% BSA. To detect signal, 0.1 ml tetramethylbenzidine (TMB) peroxidase substrate solution (Bio-Rad, Inc.) was added to each well. Plates were incubated for 30 min at room temperature before reactions were stopped by the addition of 0.1 ml 1N H_2SO_4. Signal was read and quantitated at 405 nm with an ELx800 absorbance microplate reader (Biotek, Inc., Winooski, VT).

LCM. A normal human transverse colon tissue specimen (Bioserve), obtained during a colonoscopy and immediately flash frozen, was examined by a histologist and oriented in OCT gel (Sakura Finetek USA, Inc., Torrance, CA) for sectioning to obtain optimal apical-basolateral cross sections. Tissue was sectioned (6 μM) on polyethylene naphthalate (PEN) glass membrane slides (Molecular Devices, Inc., Sunnyvale, CA), briefly thawed, and stained by a modified, abbreviated hematoxylin-eosin (H&E) staining method as follows. Thawed tissue was sequentially transferred into the following solutions: 70% ethanol (EtOH), 30 s; water, 20 s; hematoxylin, 15 s; water, 15 s; H&E Bluing solution (Sigma-Aldrich), 15 s; 70% EtoH, 15 s; eosin, 1 s; 95% EtOH, 20 s; 95% EtOH, 20 s; 100% EtOH, 20 s; 100% EtOH, 20 s; and xylene, 20 s. Slides were then air dried for 3 to 5 min. Epithelial cells from the stained tissue slides were visualized and excised with an Arcturus Pixcell II laser capture microdissection (LCM) instrument (Molecular Devices) onto LCM macro caps according to the picopure RNA isolation kit product protocol (Molecular Devices).

Quantitative real-time PCR. RNA was isolated from tissue culture cells with Trizol (Life Technologies), following the product protocol for adherent tissue culture cells. RNA was isolated from laser-excised human colon tissue with the Picopure RNA isolation kit (Molecular Devices). Total RNA was quantitated spectrophotometrically with a Nanodrop spectrophotometer (Thermo Scientific, Pittsburgh, PA). RNA quality was initially assessed spectrophotometrically through the $A_{260/280}$ ratio and later verified based on the efficiency of the real-time PCRs. Reverse transcription of the mRNA was carried out on 500 ng total RNA in 20 μl using the Transcriptor First Strand cDNA synthesis kit (Roche Applied Science, Indianapolis, IN) and the random hexamer primer included in the kit. The total RNA was denatured for 10 min at 65°C and immediately placed on ice, and then cDNA was synthesized with the following cycling program: 25°C, 10 min; 55°C, 30 min; and 85°C, 5 min. The LightCycler TaqMan master mix kit (Roche) was used to prepare quantitative real-time PCR (qRT-PCR) mixes (20 μl) for each amplicon. Reaction mixes included 300 nM Universal TaqMan probe (Roche) with 500 nM (each) primer specific for the cognate target mRNA. Universal TaqMan probes and primers used were as follows: Gb3 synthase, Universal Probe 44 (Roche); "Gb3 Left" primer, ATCCCCACCTCTCTGC AAT; "Gb3 Right" primer, CCAGATCAGACCAGGAGCTT; Gb4 synthase, Universal Probe 71 (Roche); "Gb4 Left" primer, GACCCGGTTGACCTGTTG; "Gb4 Right" primer, GCGAGCCGAAGGTTCTTT; beta-actin control, Universal Probe ACTB (Roche); "ActB Left" primer, CAACCGCGAGAAGATGAC; "ActB Right" primer, GTCCATCACGATGCCAGT; TBP control, Universal Probe TBP (Roche); "TBP Left" primer, TGAATCTTGGTTGTAAACTTG ACC; and "TBP Right" primer, CTCATGATTACCGCAGCAAA. Real-time PCRs were carried out in 20 μl glass capillary tubes in a Roche LightCycler 2.0. The cycling program used on all amplicons was as follows: 95°C for 30 s; 50 cycles of 95°C for 10 s, 55°C for 30 s, and 72°C for 1 s; and 40°C for 30 s. To generate relative and absolute values of transcript number for each sample, a standard curve was generated for each amplicon with a dilution series of cDNA plasmids for each gene. Accession numbers for these genes are as follows: *gb3 synthase* cDNA (A4GALT), accession no. BC017068 (ATCC); *gb4 synthase* cDNA (B3GALNT1), accession number BC047618 (ATCC). The LightCycler software program, version 4.1 (Roche), was used to determine absolute and relative quantities of given mRNA targets for each sample. The following controls were included in all experiments: no reverse transcriptase, no cDNA template, and a positive cDNA target. Additionally, amplification of cDNAs for the housekeeping genes that encode β-actin (ACTB) (ATCC) and TATA-binding protein (TBP) (ATCC) was run in parallel with each sample to ensure that equivalent amounts of input RNA were used in each reaction.

Cytotoxicity assays. Vero or HCT-8 cells were seeded in 96-well plates and allowed to grow for 24 h. Cytotoxicity assays were carried out as previously described for Vero cells (14). Briefly, cell monolayers were overlaid with serial dilutions of the toxin preparations and incubated for 48 h. The Vero or HCT-8 cells were then fixed in 2% formalin for 30 min, stained with 0.13% crystal violet for 2 h, washed with water, and air dried. The cell density that remained in each well was then determined spectrophotometrically. The 50% cytotoxic dose (CD_{50}) was calculated as the quantity of toxin that killed 50% of the cell monolayer.

RESULTS

Stx1 and Stx2 bind to human colonic epithelial cells. To determine whether Stx1 or Stx2 can bind to human colonic epithelial cells, normal human colon tissue sections were incubated with Stx1 or Stx2 and stained to determine toxin localization in the tissue cross section (Fig. 2A and B). Although Stx1 and Stx2 predominantly localized within the mucosal lamina propria and the surrounding submucosal vasculature, as was expected based on previous reports (48, 49), some toxin did bind to the colonic epithelial cell surface that abuts the luminal cavity (Fig. 2A and B, arrows). However, Stx1 binding was more widespread than that of Stx2 on the epithelium, lamina propria, and submucosa (Fig. 2A versus B, respectively). The finding that Stx1 and Stx2 bound discretely to the colonic epithelium surface suggested that a receptor for the toxin was present on those cells. Next, we asked whether these relative toxin binding patterns would be similar on a human colonic epithelial cell line (HCT-8). To address that question, HCT-8 cells were incubated with Stx1 or Stx2, stained, and analyzed microscopically (Fig. 2C and D) or by flow cytometry (Fig. 2E). The findings from the latter investigation were consistent with the results from the tissue sections. Both Stx1 and Stx2 bound to the surface of HCT-8 cells in a dose-dependent manner, but Stx1 was associated with a greater number of cells than was Stx2.

Gb3 and Gb4 can be detected on the surface of human colonic epithelial tissue and on a human colonic epithelial cell line. Because we observed binding of Stx to two different human colonic epithelial sections and since Gb3 is the established primary receptor for Stx, we sought to reassess the possibility that Gb3 is present on human colonic epithelia. For that purpose, we probed human colonic sections with a Gb3-specific monoclonal antibody and analyzed the sections by fluorescence microscopy (Fig. 3A). In keeping with the previous immunohistochemical analyses for Gb3 reported by others (36, 48, 49), we did not observe a positive stain for that glycosphingolipid on the epithelia. Rather, we found that Gb3 was localized to the submucosal vasculature and the capillary-rich lamina propria. A comparable pattern for the localization of Gb3 was evident on a second colonic tissue sample (data not shown). Tissues probed with an isotype-specific antibody and/or the secondary antibody alone yielded no fluorescence. Although no Gb3 was identified with the antibody probe we used, we could not rule out the possibility that Gb3 was present at low levels on the tissues, since the anti-Gb3 used has a relatively low affinity for Gb3 (unpublished observation) and in fact the affinity of the Stxs for Gb3 is likely much higher than that of the antibody.

While other glycolipids and possibly proteins (10) bind the Stxs, Gb4, a glycosphingolipid made from Gb3 (refer again to Fig. 1), is the only other well-characterized cell surface moiety capable of binding Stx1 or Stx2 (9, 20, 31, 59). Therefore, we sought to determine if colonic epithelial cells contain Gb4 on the cell surface. To this end, sections from two different human colonic samples were assessed for the presence of Gb4 with

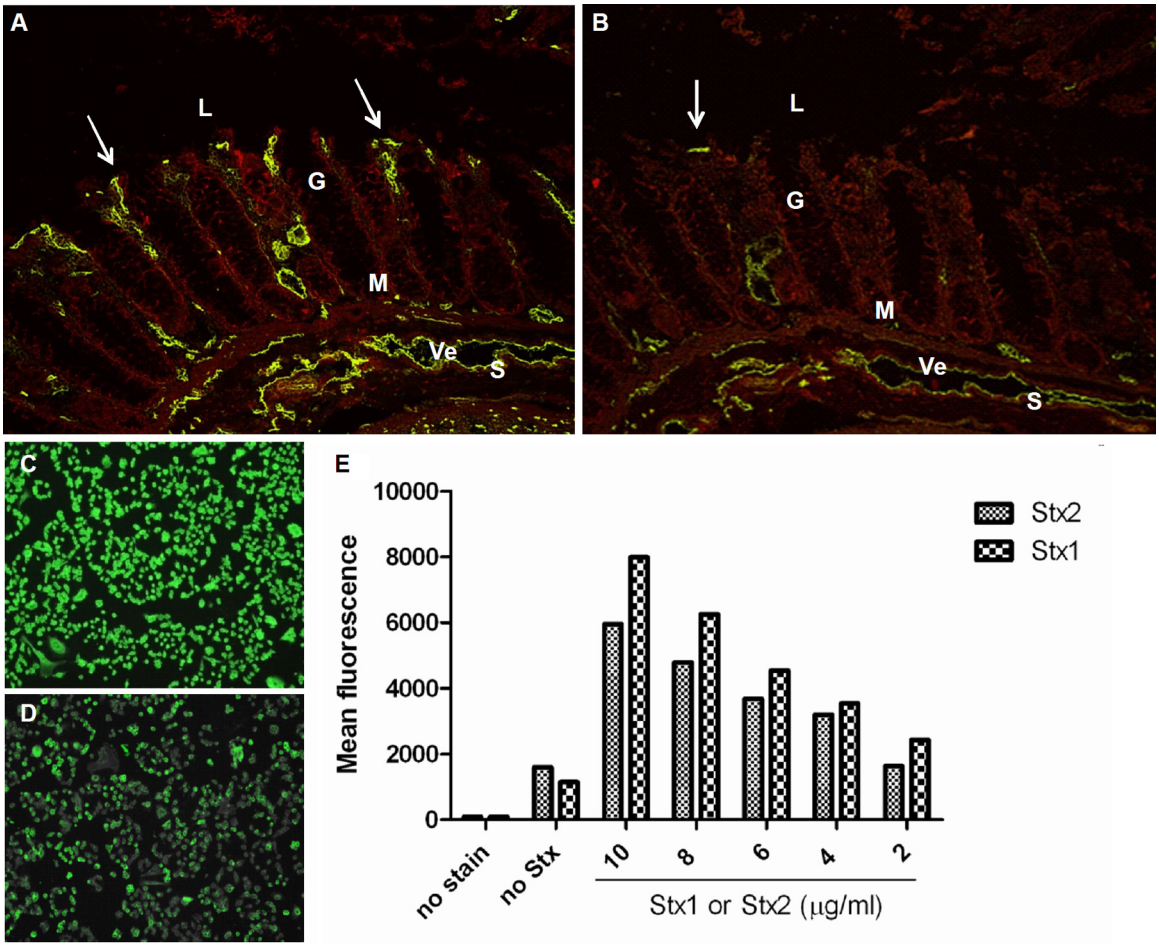

FIG. 2. Stx1 and Stx2 bind to human colonic epithelial cells. (A and B) Freshly thawed normal human colonic sections were incubated with purified Stx1 (2 μg) (A) or Stx2 (2 μg) (B), and toxin was detected with cognate mouse monoclonal primary antibody and an Alexa Fluor 488-conjugated anti-mouse IgG secondary antibody. Arrows indicate Stx binding to the epithelial surface. (C and D) HCT-8 colonic epithelial cells were incubated with purified Stx1 (200 ng/ml) (C) or Stx2 (200 ng/ml) (D), and toxin was detected as described above. (E) Binding of Stx1 and Stx2 to HCT-8 cells was quantitated by flow cytometric analyses. L, lumen; G, gland; M, muscularis mucosa; Ve, vein; S, submucosa.

polyclonal rabbit anti-Gb4 followed by incubation with a fluorescently labeled secondary antibody. The tissue showed abundant Gb4 present in a diffuse pattern on the epithelial cell surface and in the lamina propria and submucosal layers (Fig. 3B). Similar abundant and diffuse staining for Gb4 was found in a second normal human colonic section (data not shown). The finding of Gb4 in the human colonic sections supports the idea that Gb3 may also be present in those tissues, since Gb4 synthesis begins with Gb3. As a comparison to the normal human tissue sections, HCT-8 cells were similarly stained for cell surface Gb3 (Fig. 3E) and Gb4 (Fig. 3F). We found that only approximately 0.01% of the HCT-8 cells were Gb3 positive, and those positive cells occurred in small clusters (Fig. 3E). In contrast to the low levels of Gb3, the majority of HCT-8 cells stained positive for cell surface Gb4 (Fig. 3F). As expected, the secondary control antibody did not bind to the HCT-8 cells (data not shown).

Gb4 is more abundant than Gb3 in colonic epithelial cell extracts. The discovery that some HCT-8 cells were Gb3 positive was further corroborated by a positive signal for Gb3 observed by thin-layer chromatography (TLC) and mass spectrometry (MS) analysis of HPLC-purified HCT-8 cell lipid extracts (Fig. 4A and B). Of note, HCT-8 cell extracts exhibited a strong signal for Gb4 by TLC (Fig. 4A). The presence of Gb3 and Gb4 in these cells was further verified by MS of the HPLC fractions that corresponded with the Gb3- and Gb4-positive TLC bands, respectively (Fig. 4B and C).

Stx1 and Stx2 bind to purified Gb4. To compare the relative binding of Stx1 and Stx2 to Gb4, each toxin was incubated with decreasing amounts of purified Gb3 (as a control; Fig. 5A) or Gb4 adhered to wells of a 96-well microtiter plate (Fig. 5B). As anticipated from previous studies (15, 56), both Stx1 and Stx2 bound Gb3, and Stx1 bound Gb3 with a higher affinity than did Stx2. Both toxins bound to purified Gb4 at high concentrations of the glycosphingolipid, but the extent of Stx2 binding to Gb4 even at 5 μg was quite low (Fig. 5B). These data are consistent with the Stx1 and Stx2 binding patterns observed by immunofluorescent staining of human colon sections and HCT-8 cells (Fig. 2).

Gb3 synthase transcript is present in normal colonic epithelia. Despite our inability to detect Gb3 on the surface of the epithelial layer of normal human colon specimens by immu-

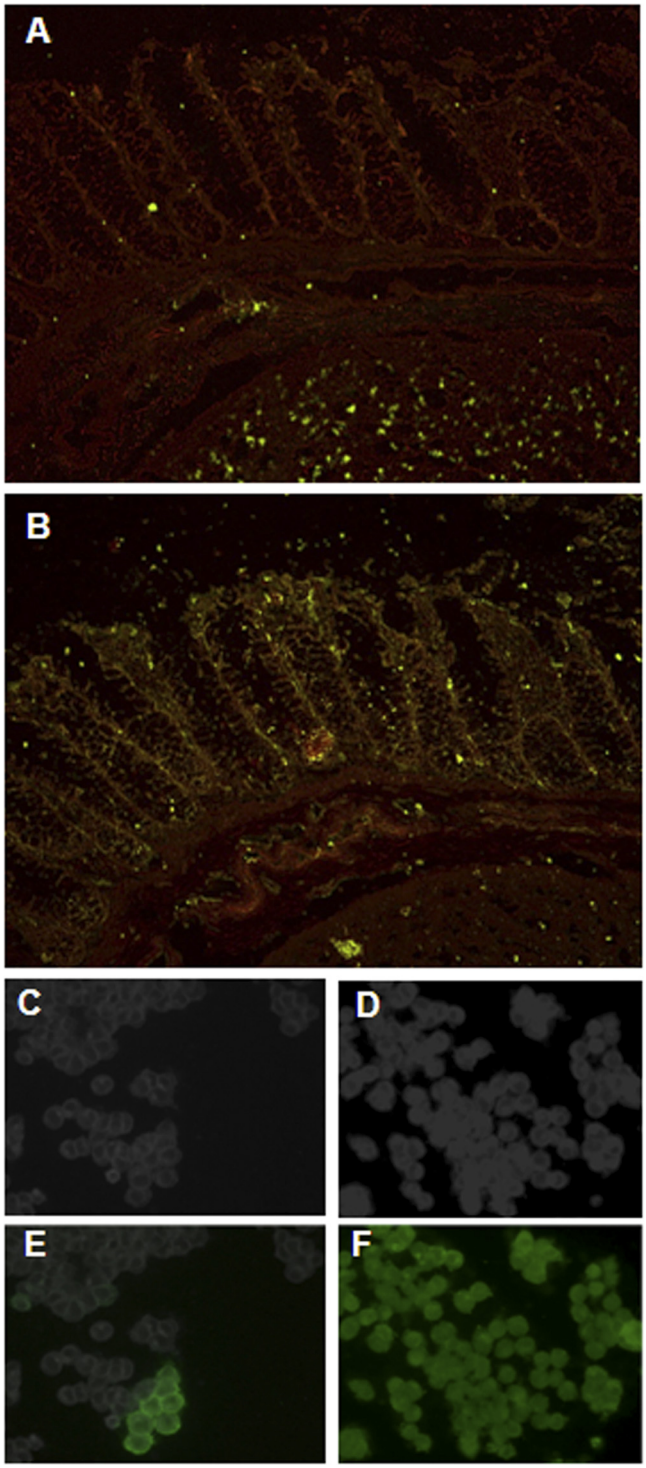

FIG. 3. Gb3 is present in the submucosal vasculature, and Gb4 is abundant on the cell surface and throughout colonic epithelial cells. Freshly thawed human colonic sections were incubated with monoclonal anti-Gb3 (A) or polyclonal anti-Gb4 (B) and stained with the appropriate secondary Alexa Fluor 488 antibody. Sections were counterstained with 0.01% Evans blue dye to accentuate tissue structure. (C to F) HCT-8 cells were grown to equivalent densities on coverslips (C and D) and were stained to detect Gb3 (E) or Gb4 (F) as described above.

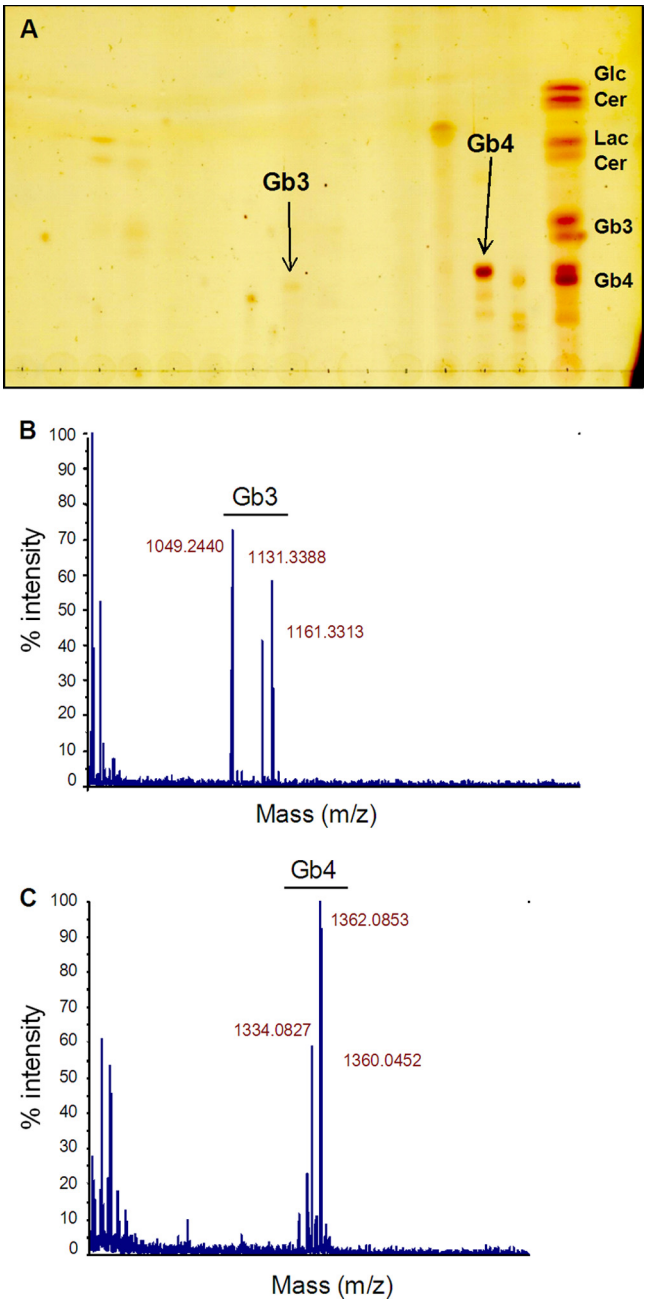

FIG. 4. Gb3 can be detected in HCT-8 cells. (A) Folch's extraction-enriched HCT-8 cellular extracts were separated by HPLC, and fractions were further separated by thin-layer chromatography with purified glycosphingolipid standards run in parallel to identify Gb3 and Gb4 species. (B and C) Mass spectrometry was carried out on the HPLC fractions that corresponded with the appropriate Gb3- and Gb4-containing samples, respectively, which were identified by TLC in panel A.

nofluorescence (Fig. 3A), we did, as noted above, detect a small percentage of colonic epithelial HCT-8 cells within a population of cells in culture that stained positive for cell-surface Gb3 (Fig. 3E). Therefore, we speculated that perhaps human tissue colonic epithelial samples actually do contain Gb3 but that the amounts of this glycolipid are below the limit

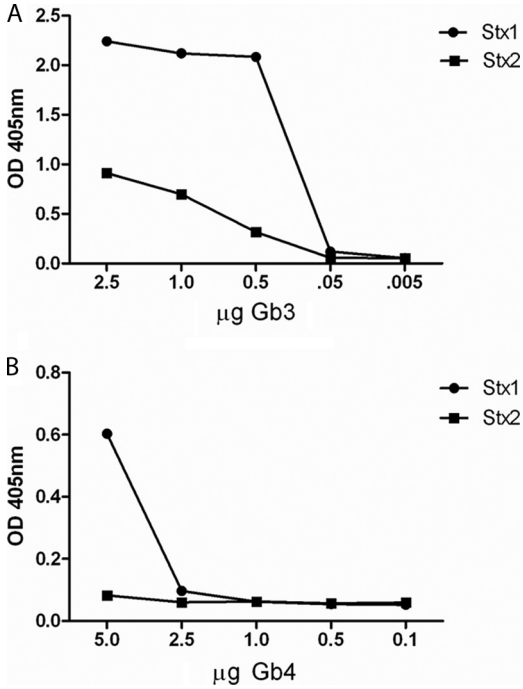

FIG. 5. Stx1 and Stx2 bind to purified Gb3 and Gb4. Stx interactions with Gb3 (A) or Gb4 (B) were determined by ELISA. Wells contained serial dilutions of the glycosphingolipids and 20 ng Stx1 or Stx2.

of detection by our immunofluorescence procedure. To test this possibility, we used the highly sensitive quantitative RT-PCR method to measure levels of Gb3 synthase transcript in human colonic epithelial tissue. Gb3 synthase generates Gb3 from lactose-ceramide (LacCer) (see synthesis scheme in Fig. 1). Laser capture microdissection was carried out on a fresh human tissue section to isolate the epithelial cells for analysis (Fig. 6A and B). The amount of Gb3 synthase transcript within the RNA isolated from the epithelia was compared to levels in the remaining tissue section (denoted "epithelium + r" in Fig. 6), the latter of which contained endothelial cells of the mucosa and submucosa, as well as other epithelial cells. Approximately 20 and 120 copies of Gb3 synthase mRNA per ng total RNA were detected in epithelial cells and the remaining tissue, respectively (Fig. 6C). By comparison, 500 copies and 811 copies of Gb3 synthase mRNA per ng total RNA were measurable in HCT-8 cells and the highly Stx-sensitive Vero cells, respectively (Fig. 6D). Surprisingly, Gb4 synthase transcript levels were lower than those of Gb3 synthase in all colonic tissues (Fig. 6C) and cells (Fig. 6D) examined. In fact, we were unable to detect Gb4 synthase transcript in the dissected colonic epithelium.

A reduction in Gb4 synthase increases cell surface Gb3 expression and enhances the sensitivity of HCT-8 cells to Stxs. Because we found Gb4 on human colonic epithelial cells and tissue sections, we next began to address whether Gb4 can bind the Stxs and then serve as a functional Stx receptor in human colonic epithelial cells. To that end, we used Gb4 synthase-specific shRNA expression (RNAi) in HCT-8 cells to produce a stable cell line in which Gb4 synthase levels were reduced.

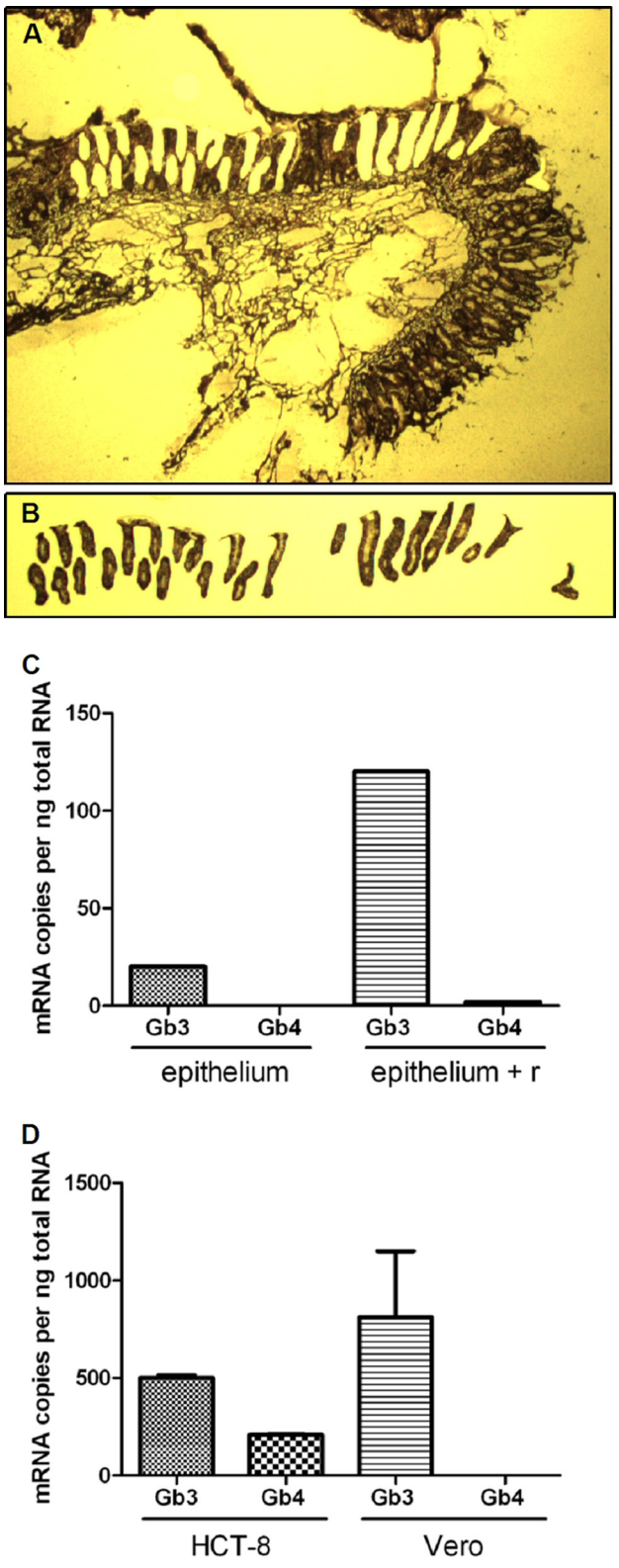

FIG. 6. Gb3 and Gb4 synthase transcripts are present in normal colonic epithelia. (A and B) A freshly thawed human colonic section was subjected to a modified H&E staining procedure to visualize tissue structure (A), followed by isolation of epithelial cells by LCM (B). (C and D) Gb3 synthase and Gb4 synthase mRNA levels in LCM-isolated epithelial cells (epithelium) and the remaining colonic section (epithelium + r) (C) or HCT-8 cells and Vero cells (D) were assessed by qRT-PCR.

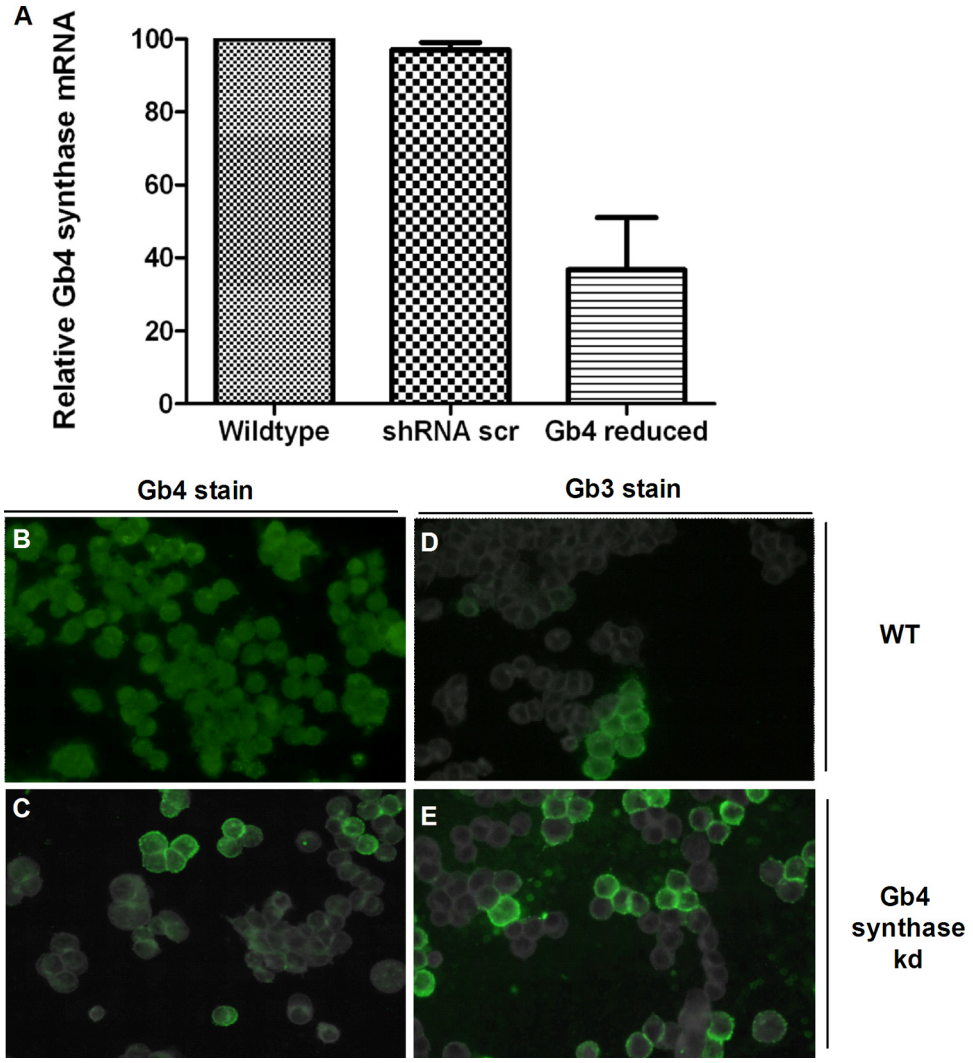

FIG. 7. Gb4 synthase RNAi knockdown decreases cell surface Gb4 expression and increases cell surface Gb3 expression. (A) A stable HCT-8 Gb4 synthase-reduced (knockdown) cell line was generated, and the Gb4 synthase transcript level was measured by qRT-PCR. (B to E) Gb3 and Gb4 cell surface levels in HCT-8 wild-type and Gb4 synthase-reduced cells were evaluated by fluorescence microscopy. Error bars represent the range of values for three experiments. Abbreviations: scr, scrambled; kd, knockdown; WT, wild type.

The HCT-8 Gb4 synthase-reduced cells expressed 50% less Gb4 synthase mRNA (compare with mRNA from HCT-8 wild-type or HCT-8 scrambled [nonspecific] shRNA-expressing cells in Fig. 7A). Immunofluorescent staining confirmed that Gb4 cell surface levels were reduced in the HCT-8 Gb4 synthase-reduced cells (Fig. 7C) compared to levels in HCT-8 wild-type cells (Fig. 7B) or scrambled shRNA-expressing control cells (not shown). Of note, Gb3 cell surface expression increased in the HCT-8 Gb4 synthase-reduced cells compared to that in the HCT-8 wild type (Fig. 7D and E).

To assess the effect of alterations in cell surface Gb4 levels on Stx binding, Stx1 or Stx2 was incubated with HCT-8 cells (Gb4 synthase-reduced cells or wild type) and then detected by fluorescence microscopy (Fig. 8). The Stx1 binding signal and distribution appeared similar in HCT-8 wild-type and Gb4 synthase-reduced cell lines (Fig. 8A versus B). However, Stx2 bound a larger percentage of wild-type HCT-8 cells in a population than it did with the Gb4 synthase-reduced cells (Fig. 8C and D). Thus, a shift in the glycosphingolipid cell surface population from high Gb4 and low Gb3 to lower Gb4 and higher Gb3 did not affect Stx1 binding but did diminish Stx2 binding.

Next, we compared the level of Stx sensitivity of the HCT-8 Gb4 synthase-reduced cells to that of the HCT-8 wild-type or scrambled shRNA-expressing cells and that of Vero cells (Table 1). In the HCT-8 cells with reduced Gb4 synthase, the cytotoxicity of both Stx1 and Stx2 increased to levels comparable to those in the highly Stx-sensitive Vero cells as measured by a decrease in the amount of toxin needed to kill 50% of cells (the CD_{50}). Regardless of the Gb3 levels in the HCT-8 cells, Stx2 was less cytotoxic for the cells than was Stx1. This relative difference in Stx1 and Stx2 cytotoxicities has previously been observed with Vero cells (54). We propose that the enhanced Stx sensitivity of the HCT-8 cell line with reduced Gb4 synthase is due to the increased Gb3 levels on those cells.

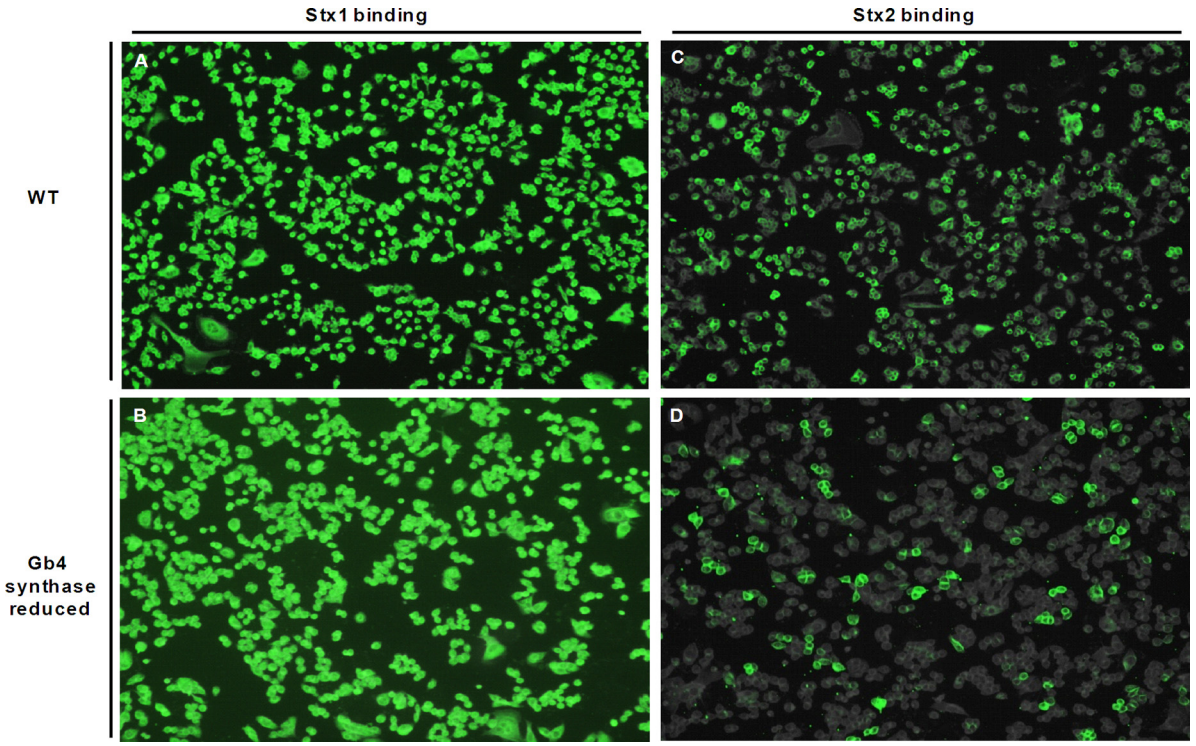

FIG. 8. Stx2 binding to HCT-8 Gb4 synthase-reduced cells is decreased compared to that to HCT-8 wild-type cells. HCT-8 wild-type and Gb4 synthase-reduced cells were intoxicated with 200 ng/ml Stx1 (A and B) or Stx2 (C and D), and toxin was detected with cognate mouse monoclonal antibody and an Alexa Fluor 488-conjugated anti-mouse IgG antibody.

DISCUSSION

In this investigation, we demonstrated for the first time that Stx1 and Stx2 could bind to the surface of colonic epithelial cells in fresh human tissue sections and that Stx1 bound to this surface at more locations than did Stx2. Similarly, we showed that both toxins bound colonic epithelial cells (HCT-8) in culture and that Stx1 did so more extensively than did Stx2. In addition, we presented the novel findings that human colonic tissues and HCT-8 cells produce Gb3 synthase transcript and express cell surface Gb4. Moreover, we discovered that Gb3 was expressed on the surface of a small subset of HCT-8 cells. Last, we found that a reduction in the expression of Gb4 synthase in HCT-8 cells resulted in an increase in cell surface Gb3 and a concomitant increase in sensitivity of those cells to both Stx1 and Stx2.

We hypothesize that binding of Stx to the surface of normal human colonic epithelium has not previously been reported because of several possible factors. First, the amount of toxin used as a probe in prior studies may have been suboptimal for detection of the small amount of toxin bound to the epithelium compared to that for the endothelium. In this study, 2 μg toxin was applied to tissue sections, which is approximately a 10-fold-greater amount than that used previously (48). Second, we theorize that visualization of epithelial-surface binding by Stx may be difficult to discern against the background of a strong signal from the endothelium and/or that more-abundant/accessible binding sites within the endothelium outcompete the relatively few sites on the epithelial surface. Third, because colonic tissue is especially susceptible to rapid degradation outside of the host (18), Stx receptors may have been destroyed during tissue collection in prior investigations. For our Stx binding studies, the normal colonic tissue used was obtained during biopsy and was flash frozen, a procedure that likely minimized tissue degradation. Finally, variations in Stx binding sites on the colonic epithelium may exist among different specimens. We note, however, that the binding of Stx to the epithelium in our investigation was detected in similar amounts and localization in two different colonic tissue specimens.

While we did not directly detect Gb3 on the surface of human colonic epithelia in tissue sections, we hypothesize that at least some of these cells harbor cell surface Gb3, based on the following observations. In HCT-8 cells, in which a subset of the population stains positive for Gb3, and in isolated colonic epithelial cells, we detected Gb3 synthase transcript. Likewise, both in HCT-8 cells and in isolated colonic epithelial cells,

TABLE 1. Gb4 synthase RNAi knockdown HCT-8 cell line is sensitized to Stx1 and Stx2

Cell line[a]	CD_{50}[b] (pg)	
	Stx1	Stx2
Vero	18	35
HCT-8	80	480
HCT-8 scr.	60	1,000
HCT-8 ↓	1	48

[a] HCT-8 scr., scrambled shRNA-containing cells; HCT-8 ↓, Gb4 synthase-reduced cells.
[b] CD_{50}, dose required to kill 50% of the cell monolayer.

similar strong staining of the Gb3 precursor, Gb4, was observed. Further, the sensitivity of HCT-8 cells to Stxs (Table 1), given the limited detection of Gb3 in these cells (Fig. 3), suggests a broader proportion of subdetectable cell surface Gb3 content. The possibility that a non-Gb3 receptor mediates these cytotoxic effects is unlikely, since we observed a marked increase in Stx1 and Stx2 sensitivity in Gb4 synthase-reduced HCT-8 cells that have increased cell surface Gb3 levels (Fig. 7 and Table 1). Further support for our hypothesis that Gb3 is present in fresh sections of human colonic epithelia is that Gb3 is present on the gastrointestinal mucosa of both rabbits and mice, two animals that are also susceptible to the effects of the toxin (25, 28, 37). Our data suggest that in the colonic epithelia, glycosphingolipid synthesis kinetics appear to drive high levels of Gb4 production, which, we speculate, effectively limits the amount of detectable Gb3.

Our observation of abundant Gb4 on the surface of normal human colonic epithelial sections and on HCT-8 cells in culture initially suggested to us that Gb4 might function as an alternate Stx receptor on the surface of the colon, since Stx1 and Stx2 are both known to bind to Gb4, albeit with lower affinity than that for Gb3 (35). In support of a positive Gb4-Stx interaction on the colonic epithelium, we observed a dose-dependent binding of Stx1 and Stx2 to HCT-8 cells in a pattern similar to the distribution of Gb4 staining. However, our data that showed a striking increase in the cytotoxicities of Stx1 (60-fold) and Stx2 (20-fold) for the HCT-8 cells (Table 1) with reduced Gb4 synthase compared to those for control HCT-8 cells with scrambled shRNA (Table 1) suggest that Gb4 is in fact not acting as a functional receptor for either Stx1 or Stx2. Rather, these results, along with the increase in cell surface Gb3 on the Gb4 synthase-reduced HCT-8 cells (Fig. 7), strongly indicate that Gb3 is the primary functional receptor for Stxs on colonic epithelial cells and suggest that Gb4 may bind the toxins without a cytotoxic consequence. Our finding that Stx2 did not bind more strongly to the HCT-8 Gb4 synthase-reduced cell line but was more toxic to those cells is additional evidence that for the Stxs, cell surface binding does not correlate completely with cytotoxicity. Furthermore, the reduced binding of Stx2 in the Gb4 synthase-reduced HCT-8 cell line likely reflects a loss of Gb4-Stx2 interaction.

We observed that more Stx1 than Stx2 bound to purified Gb3 and Gb4, to HCT-8 cells, and to colonic tissue sections. We noted, as have others (56), that both Stx1 and Stx2 bound less well to Gb4 than they did to Gb3, but we found that Stx2 in particular did not bind well to Gb4 in the ELISA format. We suspect that the differences in binding of Stx2 to purified Gb3 and Gb4 in the ELISA, compared to its interaction with HCT-8 cells, reflect a preference of Stx2 for the cell surface arrangement of Gb3 and Gb4. Lingwood's group has shown that the Stxs prefer to bind to glycosphingolipids (GSLs) that are present in lipid rafts and that the fatty acid chain length also plays a role in how well the toxins bind to subsets of Gb3 (8, 54). Furthermore, such a preference for Stx1 and Stx2 binding to selected subsets of GSLs may explain why the patterns of staining for Stxs (Fig. 2) were discrete compared to the diffuse pattern of Gb4 detection by antibody (Fig. 3).

We were surprised to find that Gb4 synthase transcript levels in HCT-8 cells and normal human colon tissue were significantly lower than would be expected based on Gb4 immunostaining. Despite our ability to accurately amplify Gb4 synthase cDNA from a plasmid, multiple experiments yielded the same low-level Gb4 synthase transcript amounts in HCT-8 cells and undetectable levels in Vero cells. Two possible hypotheses that may explain the low levels of Gb4 synthase transcript yet high levels of Gb4 we observe include an unstable Gb4 synthase transcript and/or a stable and/or efficient Gb4 synthase protein. An analysis of the sequence of Gb4 synthase revealed the presence of mRNA-destabilizing properties that are not present in Gb3 synthase mRNA. Indeed, throughout the lengthy 3′ untranscribed region (3′-UTR) (1,906 nucleotides [nt]; average 3′-UTR is 740 nt) of the Gb4 synthase transcript, multiple mRNA-destabilizing elements are present. Notably, two destabilizing nonameric AU-rich elements (ARE and UUAUUUAUU) are located within the 500 nucleotides proximal to the stop codon within the Gb4 synthase mRNA. Two or more copies of this motif are associated with a short-lived mRNA half-life (30). In addition to the nonameric ARE sequence, at least four copies of the well-characterized ARE element AUUUA are present within the 3′-UTR of the Gb4 synthase mRNA. In contrast to the numerous potential destabilizing elements within the Gb4 synthase mRNA 3′-UTR, the Gb3 synthase transcript is devoid of any such ARE elements. Therefore, the detection of only low levels of Gb4 synthase mRNA is likely due to instability of the transcript. In addition, the Gb4 synthase protein is predicted to be stable, while the Gb3 synthase protein is most likely unstable, according to an analysis by the ProtParam protein algorithm (13). Alternatively, a mechanism of negative autoregulation of Gb3 synthase transcription by Gb3 synthase itself (directly or indirectly) would also explain these data. Negative autoregulatory mechanisms that limit the transcript amount in this manner have been described (3). Taken together, our analysis suggests that Gb4 synthase efficiently drives the production of Gb4 from the available cellular Gb3 substrate in normal colonic tissue and in HCT-8 cells. Moreover, a kinetically favorable production of Gb4 from Gb3 would explain the relatively low levels of Gb3 we observe in cells and in colonic tissue sections. Why this regulatory mechanism would differ between Gb3 synthase and Gb4 synthase is not immediately apparent.

Overall, our data suggest a model in which small amounts of Gb3 are expressed on the surface of the colonic epithelia among abundant Gb4. We predict that Stx binding to colonic epithelial cells occurs through both receptors. Although we did not observe identical patterns of immunofluorescence for localization of the Stxs versus Gb3 and Gb4 on the tissue sections, those differences in staining patterns most likely occur because the Stxs bind better to certain subsets of Gb3 and Gb4 (8). In addition, we suggest that whereas the interaction of Stx with Gb3 results in a functional toxic event, binding to Gb4 does not and may lead to a sequestration of the toxin. The implication that Gb3 is present on a subset of cells within the colonic epithelial surface is significant because it suggests a possible mechanism for Stx penetration of the epithelia. Stx-generated apoptosis of some cells in the epithelial barrier may allow the toxin access to the lamina propria and the associated vasculature through a temporary lesion in the epithelium. The toxin may then damage the Gb3-rich colonic endothelial cells and lead to hemorrhagic colitis or, in a worst-case scenario, systemic toxemia and the HUS. Because Stx1 binds to Gb4 at

higher levels than does Stx2, the reason that Stx1 expression by STEC is less likely to lead to the HUS may be that Stx1 is bound to the Gb4 present in the gut, such that less of the toxin binds to the functional receptor Gb3 to cause toxicity. However, because we also observed that Stx2 bound to Gb4 on HCT-8 cells, in some cases without cytotoxicity, it may be that the balance of Gb3 and Gb4 within the gut in an individual host plays a role in whether that person develops the HUS.

ACKNOWLEDGMENTS

We thank Stephen Darnell for purification of Stx1 and Stx2 and Edda Twiddy for maintenance of Vero cells used in cytotoxicity assays. We additionally thank Krystle Mohawk for technical expertise with the ELISA and Christy Ventura for contributions to manuscript editing.

This work was supported by grants AI57168 and AI20148 from the National Institutes of Health.

REFERENCES

1. **Acheson, D. W., R. Moore, S. De Breucker, L. Lincicome, M. Jacewicz, E. Skutelsky, and G. T. Keusch.** 1996. Translocation of Shiga toxin across polarized intestinal cells in tissue culture. Infect. Immun. **64:**3294–3300.
2. **Ahn, C. K., N. J. Holt, and P. I. Tarr.** 2009. Shiga-toxin producing *Escherichia coli* and the hemolytic uremic syndrome: what have we learned in the past 25 years? Adv. Exp. Med. Biol. **634:**1–17.
3. **Bateman, E.** 1998. Autoregulation of eukaryotic transcription factors. Prog. Nucleic Acid Res. Mol. Biol. **60:**133–168.
4. **Beery, J., M. Doyle, and N. Higley.** 1984. Cytotoxic activity of *Escherichia coli* O157:H7 culture filtrate on the mouse colon and kidney. Curr. Microbiol. **11:**335–342.
5. **Berky, J. J., J. Hunziker, Jr., and L. A. Zolotor.** 1981. Laboratory apparatus for cloning mammalian cells. U.S. patent 4247646.
6. **Bitzan, M.** 2009. Treatment options for HUS secondary to *Escherichia coli* O157:H7. Kidney Int. Suppl. **2009:**S62–S66.
7. **Boyd, B., and C. Lingwood.** 1989. Verotoxin receptor glycolipid in human renal tissue. Nephron **51:**207–210.
8. **Boyd, B., G. Magnusson, Z. Zhiuyan, and C. A. Lingwood.** 1994. Lipid modulation of glycolipid receptor function. Availability of Gal(alpha 1-4)Gal disaccharide for verotoxin binding in natural and synthetic glycolipids. Eur. J. Biochem. **223:**873–878.
9. **DeGrandis, S., H. Law, J. Brunton, C. Gyles, and C. A. Lingwood.** 1989. Globotetraosylceramide is recognized by the pig edema disease toxin. J. Biol. Chem. **264:**12520–12525.
10. **Devenish, J., C. Gyles, and J. LaMarre.** 1998. Binding of *Escherichia coli* verotoxins to cell surface protein on wild-type and globotriaosylceramide-deficient Vero cells. Can. J. Microbiol. **44:**28–34.
11. **Flagler, M. J., S. S. Mahajan, A. A. Kulkarni, S. S. Iyer, and A. A. Weiss.** 2010. Comparison of binding platforms yields insights into receptor binding differences between shiga toxins 1 and 2. Biochemistry **49:**1649–1657.
12. **Forzley, B. R., and W. F. Clark.** 2009. TTP/HUS and prognosis: the syndrome and the disease(s). Kidney Int. Suppl. **2009:**S59–S61.
13. **Gasteiger, E., A. Gattiker, C. Hoogland, I. Ivanyi, R. D. Appel, and A. Bairoch.** 2003. ExPASy: the proteomics server for in-depth protein knowledge and analysis. Nucleic Acids Res. **31:**3784–3788.
14. **Gentry, M. K., and J. M. Dalrymple.** 1980. Quantitative microtiter cytotoxicity assay for Shigella toxin. J. Clin. Microbiol. **12:**361–366.
15. **Head, S. C., M. A. Karmali, M. E. Roscoe, M. Petric, N. A. Strockbine, and I. K. Wachsmuth.** 1988. Serological differences between verocytotoxin 2 and shiga-like toxin II. Lancet **ii:**751.
16. **Holgersson, J., P. A. Jovall, and M. E. Breimer.** 1991. Glycosphingolipids of human large intestine: detailed structural characterization with special reference to blood group compounds and bacterial receptor structures. J. Biochem. **110:**120–131.
17. **Holgersson, J., N. Stromberg, and M. E. Breimer.** 1988. Glycolipids of human large intestine: difference in glycolipid expression related to anatomical localization, epithelial/non-epithelial tissue and the ABO, Le and Se phenotypes of the donors. Biochimie **70:**1565–1574.
18. **Huckenbeck, W.** 2006. Forensic pathology reviews, vol. 4. Humana Press, Totowa, NJ.
19. **Hughes, A. K., P. K. Stricklett, D. Schmid, and D. E. Kohan.** 2000. Cytotoxic effect of Shiga toxin-1 on human glomerular epithelial cells. Kidney Int. **57:**2350–2359.
20. **Jacewicz, M., H. Clausen, E. Nudelman, A. Donohue-Rolfe, and G. T. Keusch.** 1986. Pathogenesis of shigella diarrhea. XI. Isolation of a shigella toxin-binding glycolipid from rabbit jejunum and HeLa cells and its identification as globotriaosylceramide. J. Exp. Med. **163:**1391–1404.
21. **Jacewicz, M. S., D. W. Acheson, D. G. Binion, G. A. West, L. L. Lincicome, C. Fiocchi, and G. T. Keusch.** 1999. Responses of human intestinal microvascular endothelial cells to Shiga toxins 1 and 2 and pathogenesis of hemorrhagic colitis. Infect. Immun. **67:**1439–1444.
22. **Jones, D. H., C. A. Lingwood, K. R. Barber, and C. W. Grant.** 1997. Globoside as a membrane receptor: a consideration of oligosaccharide communication with the hydrophobic domain. Biochemistry **36:**8539–8547.
23. **Kannagi, R., K. Watanabe, and S. Hakomori.** 1987. Isolation and purification of glycosphingolipids by high-performance liquid chromatography. Methods Enzymol. **138:**3–12.
24. **Karmali, M. A.** 1989. Infection by verocytotoxin-producing *Escherichia coli*. Clin. Microbiol. Rev. **2:**15–38.
25. **Kashiwamura, M., K. Kurohane, T. Tanikawa, A. Deguchi, D. Miyamoto, and Y. Imai.** 2009. Shiga toxin kills epithelial cells isolated from distal but not proximal part of mouse colon. Biol. Pharm. Bull. **32:**1614–1617.
26. **Kelly, J., A. Oryshak, M. Wenetsek, J. Grabiec, and S. Handy.** 1990. The colonic pathology of *Escherichia coli* O157:H7 infection. Am. J. Surg. Pathol. **14:**87–92.
27. **Keusch, G. T., M. Jacewicz, D. W. Acheson, A. Donohue-Rolfe, A. V. Kane, and R. H. McCluer.** 1995. Globotriaosylceramide, Gb3, is an alternative functional receptor for Shiga-like toxin 2e. Infect. Immun. **63:**1138–1141.
28. **Keusch, G. T., M. Jacewicz, M. Mobassaleh, and A. Donohue-Rolfe.** 1991. Shiga toxin: intestinal cell receptors and pathophysiology of enterotoxic effects. Rev. Infect. Dis. **13**(Suppl. 4)**:**S304–S310.
29. **Kovbasnjuk, O.** 2005. New insights into the role of Shiga toxins in intestinal disease. Gastroenterology **129:**1354–1355.
30. **Lai, W. S., D. M. Carrick, and P. J. Blackshear.** 2005. Influence of nonameric AU-rich tristetraprolin-binding sites on mRNA deadenylation and turnover. J. Biol. Chem. **280:**34365–34377.
31. **Lindberg, A. A., J. E. Brown, N. Stromberg, M. Westling-Ryd, J. E. Schultz, and K. A. Karlsson.** 1987. Identification of the carbohydrate receptor for Shiga toxin produced by *Shigella dysenteriae* type 1. J. Biol. Chem. **262:**1779–1785.
32. **Lingwood, C. A.** 1996. Role of verotoxin receptors in pathogenesis. Trends Microbiol. **4:**147–153.
33. **Lingwood, C. A.** 2003. Shiga toxin receptor glycolipid binding. Pathology and utility. Methods Mol. Med. **73:**165–186.
34. **Lingwood, C. A.** 1994. Verotoxin-binding in human renal sections. Nephron **66:**21–28.
35. **Lingwood, C. A., H. Law, S. Richardson, M. Petric, J. L. Brunton, S. De Grandis, and M. Karmali.** 1987. Glycolipid binding of purified and recombinant *Escherichia coli* produced verotoxin in vitro. J. Biol. Chem. **262:**8834–8839.
36. **Miyamoto, Y., M. Iimura, J. B. Kaper, A. G. Torres, and M. F. Kagnoff.** 2006. Role of Shiga toxin versus H7 flagellin in enterohaemorrhagic *Escherichia coli* signalling of human colon epithelium in vivo. Cell Microbiol. **8:**869–879.
37. **Mobassaleh, M., O. Koul, K. Mishra, R. H. McCluer, and G. T. Keusch.** 1994. Developmentally regulated Gb3 galactosyltransferase and alpha-galactosidase determine Shiga toxin receptors in intestine. Am. J. Physiol. **267:**G618–G624.
38. **Muthing, J., C. H. Schweppe, H. Karch, and A. W. Friedrich.** 2009. Shiga toxins, glycosphingolipid diversity, and endothelial cell injury. Thromb. Haemost. **101:**252–264.
39. **O'Brien, A. D., and A. R. Melton-Celsa.** 2000. Handbook of experimental pharmacology, vol. 145. Springer-Verlag, Berlin, Germany.
40. **Obrig, T. G., C. B. Louise, C. A. Lingwood, B. Boyd, L. Barley-Maloney, and T. O. Daniel.** 1993. Endothelial heterogeneity in Shiga toxin receptors and responses. J. Biol. Chem. **268:**15484–15488.
41. **O'Loughlin, E. V., and R. M. Robins-Browne.** 2001. Effect of Shiga toxin and Shiga-like toxins on eukaryotic cells. Microbes Infect. **3:**493–507.
42. **Ohmi, K., N. Kiyokawa, T. Takeda, and J. Fujimoto.** 1998. Human microvascular endothelial cells are strongly sensitive to Shiga toxins. Biochem. Biophys. Res. Commun. **251:**137–141.
43. **Okuda, T., N. Tokuda, S. Numata, M. Ito, M. Ohta, K. Kawamura, J. Wiels, T. Urano, O. Tajima, and K. Furukawa.** 2006. Targeted disruption of Gb3/CD77 synthase gene resulted in the complete deletion of globo-series glycosphingolipids and loss of sensitivity to verotoxins. J. Biol. Chem. **281:**10230–10235.
44. **Pai, C. H., J. K. Kelly, and G. L. Meyers.** 1986. Experimental infection of infant rabbits with verotoxin-producing *Escherichia coli*. Infect. Immun. **51:**16–23.
45. **Perera, L. P., L. R. Marques, and A. D. O'Brien.** 1988. Isolation and characterization of monoclonal antibodies to Shiga-like toxin II of enterohemorrhagic *Escherichia coli* and use of the monoclonal antibodies in a colony enzyme-linked immunosorbent assay. J. Clin. Microbiol. **26:**2127–2131.
46. **Ren, J., I. Utsunomiya, K. Taguchi, T. Ariga, T. Tai, Y. Ihara, and T. Miyatake.** 1999. Localization of verotoxin receptors in nervous system. Brain Res. **825:**183–188.
47. **Richardson, S. E., T. A. Rotman, V. Jay, C. R. Smith, L. E. Becker, M. Petric, N. F. Olivieri, and M. A. Karmali.** 1992. Experimental verocytotoxemia in rabbits. Infect. Immun. **60:**4154–4167.
48. **Schuller, S., G. Frankel, and A. D. Phillips.** 2004. Interaction of Shiga toxin from *Escherichia coli* with human intestinal epithelial cell lines and explants: Stx2 induces epithelial damage in organ culture. Cell Microbiol. **6:**289–301.

49. **Schuller, S., R. Heuschkel, F. Torrente, J. B. Kaper, and A. D. Phillips.** 2007. Shiga toxin binding in normal and inflamed human intestinal mucosa. Microbes Infect. **9:**35–39.
50. **Shimizu, T., T. Sato, S. Kawakami, T. Ohta, M. Noda, and T. Hamabata.** 2007. Receptor affinity, stability and binding mode of Shiga toxins are determinants of toxicity. Microb. Pathog. **43:**88–95.
51. **Shin, I. S., S. Ishii, J. S. Shin, K. I. Sung, B. S. Park, H. Y. Jang, and B. W. Kim.** 2009. Globotriaosylceramide (Gb3) content in HeLa cells is correlated to Shiga toxin-induced cytotoxicity and Gb3 synthase expression. BMB Rep. **42:**310–314.
52. **Siddiqui, B., J. S. Whitehead, and Y. S. Kim.** 1978. Glycosphingolipids in human colonic adenocarcinoma. J. Biol. Chem. **253:**2168–2175.
53. **Smith, M. J., H. M. Carvalho, A. R. Melton-Celsa, and A. D. O'Brien.** 2006. The 13C4 monoclonal antibody that neutralizes Shiga toxin Type 1 (Stx1) recognizes three regions on the Stx1 B subunit and prevents Stx1 from binding to its eukaryotic receptor globotriaosylceramide. Infect. Immun. **74:**6992–6998.
54. **Tam, P., R. Mahfoud, A. Nutikka, A. A. Khine, B. Binnington, P. Paroutis, and C. Lingwood.** 2008. Differential intracellular transport and binding of verotoxin 1 and verotoxin 2 to globotriaosylceramide-containing lipid assemblies. J. Cell. Physiol. **216:**750–763.
55. **te Loo, D. M., L. A. Monnens, T. J. van Der Velden, M. A. Vermeer, F. Preyers, P. N. Demacker, L. P. van Den Heuvel, and V. W. van Hinsbergh.** 2000. Binding and transfer of verocytotoxin by polymorphonuclear leukocytes in hemolytic uremic syndrome. Blood **95:**3396–3402.
56. **Tesh, V. L., J. A. Burris, J. W. Owens, V. M. Gordon, E. A. Wadolkowski, A. D. O'Brien, and J. E. Samuel.** 1993. Comparison of the relative toxicities of Shiga-like toxins type I and type II for mice. Infect. Immun. **61:**3392–3402.
57. **van Echten, G., and K. Sandhoff.** 1993. Ganglioside metabolism. Enzymology, topology, and regulation. J. Biol. Chem. **268:**5341–5344.
58. **Waddell, T., A. Cohen, and C. A. Lingwood.** 1990. Induction of verotoxin sensitivity in receptor-deficient cell lines using the receptor glycolipid globotriosylceramide. Proc. Natl. Acad. Sci. U. S. A. **87:**7898–7901.
59. **Waddell, T., S. Head, M. Petric, A. Cohen, and C. Lingwood.** 1988. Globotriosyl ceramide is specifically recognized by the *Escherichia coli* verocytotoxin 2. Biochem. Biophys. Res. Commun. **152:**674–679.
60. **Wen, S. X., L. D. Teel, N. A. Judge, and A. D. O'Brien.** 2006. A plant-based oral vaccine to protect against systemic intoxication by Shiga toxin type 2. Proc. Natl. Acad. Sci. U. S. A. **103:**7082–7087.
61. **Whyte, D. A., and R. N. Fine.** 2008. Acute renal failure in children. Pediatr. Rev. **29:**297, 299–306.

Editor: J. B. Bliska